Influence of degradation at the base of a support post in a collapse of an old guardrail: A forensic analysis

Luca Sgambi *

Department of Civil and Environmental Engineering, Politecnico di Milano, Milan, Italy

Received 6 March 2014
Accepted 4 April 2014
Available online 18 April 2014

1. Introduction

Following a violent impact caused by a car, the guardrail installed as protection for a narrow curve in entrance of a bridge collapsed, causing the vehicle to veer off the road. Later, the vehicle continued its trajectory through the air, falling from the bridge, crashing down a slope and stopping in the bed of the stream below. The accident caused the death of the driver and the serious injury of a passenger. Given the presence of severe corrosion at the base of a number of support guardrail posts, in the forensic analysis it was necessary to study the influence of structural degradation on the mechanical behaviour and on the guardrail collapse.

The guardrail is a protective element that is placed at the sides of roads to ensure the safety of persons in case of loss of control of the vehicle. Today the design and the placement of guardrails on the roads are carried out taking into account several factors such as the potential crash severities, traffic exposure, and costs of treatment [19,35].

The method of designing a guardrail, as the design of any structural system, underwent significant changes over time, being updated according to experience and to the developments of new research. From a design based solely on the structural strength, a design was slowly developed based on the evaluation of further performance of structure and energy dissipation. Today, the performance-based design is accepted as current methodology of design and is continuously updated according to new needs originated from the society [7,9,25,6,8].

The innovation of the design methods is particularly important with regard to the design of structures subjected to dynamic loads, such as seismic action. From a design based on the concepts of resistance, we moved to a design based on

* Tel.: +39 0223994212.
E-mail address: luca.sgambi@polimi.it

the concept of energy dissipation [36]. A very similar notion is applied to the design of the guardrail. The first design methods were based on the unique concept of strength of the barrier and tried to prevent the vehicle from veering off the road. To obtain this result the horizontal guardrail beams were sized such as to be able to deform in the field of large displacements, braking and holding with a "rope effect" the running of the vehicle. With the increasing speed of vehicles and the increase of heavy traffic on the road, this mode of design showed a number of limits since, increasing the strength of the barrier, a similar increase in the probability of survival of the occupants of the impacting vehicle was not obtained. In fact, exceeding a certain threshold of resistance it is possible to ensure the remaining of the vehicle on the road but there is a decrease in the probability of survival due to the severity of the impact [14,21]. Therefore, the design of the guardrail was changed, also on the basis of considerable experimental and numerical research that has taken place over recent decades [3,4,38,17,30,23,5]. From a concept of strength we passed, in a similar manner to seismic engineering, to a concept of energy dissipation [11] and to a performance-based design in which, in addition to the strength of the guardrail, we had also to take into account the safety of the persons involved and the diversity of possible impacting vehicles [18,12,22]. These concepts led to a change in the geometry of guardrails, of which the most evident are: the section of the horizontal beam evolves from one to three waves, support posts are today much closer to each other and equipped with devices capable of dissipating energy, etc.

The subject of the correct design of a guardrail was therefore extremely contemporary and concerned research programs in many universities [29,26,27,28,37] as well as regulatory committees [1,15,16].

Most of the studies present in the literature, both experimental and numerical, analyse the guardrail in its design conditions. However, a guardrail must have a very long life cycle and must maintain its characteristics unchanged over time. The atmosphere and the salt used on the roads during the winter can trigger corrosion phenomena on the structure of the guardrail, putting at risk its functionality [20]. And in fact it has been shown that, in certain structures, the presence of corrosion can not only reduce the strength capacity of the structure but can also lead to a change in the behaviour of collapse [32–34]. Corrosion may also lead to a decrease in structural strength, causing a progressive collapse of the structure similar to that which can occur in a suspension bridge after the collapse of a suspension cable [13,24].

The case analysed in this paper relates to an incident involving a guardrail with strong signs of structural deterioration (Fig. 1). The guardrail was installed in 1970 for the protection of road traffic on a bridge located in a mountainous area. To access the bridge the road makes a sharp bend where a speed limit of 30 km/h was imposed to prevent the loss of control of the vehicle on a curve.

Probably because of the anti-freeze salts used in winter to prevent the formation of ice on the roadway and the lack of an adequate system of collection and distribution of rainwater, the base of certain guardrail posts had heavily corroded over the years.

On one night in 2008 a vehicle, moving at high speed, lost control at the entrance curve to the bridge and violently impacted against the guardrail causing it to collapse. In this manner the vehicle broke down the safety barrier, falling from the bridge and subsequently impacting on the slope of the mountain below, until it ended its run in the river bed 30 m below the roadway. The accident caused the death of the driver and the serious wounding of a second passenger.

The purpose of the forensic engineering analysis was to determine the influence of the state of deterioration of the support posts on the dynamics of the accident and whether any maintenance might have prevented the vehicle from veering off from the road, thus saving a human life.

The precise assessment of the state of deterioration of posts seemed immediately to be very difficult and uncertain. In fact, if it is evident that the posts have deteriorated significantly over time, with the posts involved in the accident it is not clear how much the lack of material was due to the corrosive process or to the impact with the vehicle that violently sheared two of them at their base. Therefore, in order to thoroughly examine the failure occurred, we started to analyse the following points:

- The qualitative reconstruction of the dynamics of the impact with identification of the mechanism of collapse.
- The quantitative assessment of the dynamics of the impact, assuming a conventional state of strong deterioration.
- The quantitative assessment of the dynamics of the impact, assuming an absence of deterioration.
- The quantitative assessment of the resistance that the guardrail was supposed to have had to stop the vehicle.
- A comparison between the results obtained.

In the following pages the points listed above will be developed, starting from the qualitative reconstruction of the impact. Throughout the process of analysis, the qualitative analysis is the most important part because it will serve as a guide in the quantitative assessment of the dynamics. The reconstruction of the impact will have to be able to explain the final position of the vehicle, the noticeable plastic deformations observed on the guardrail after the accident, the traces of braking on asphalt, the collapse mechanism and the ultimate strength of the guardrail.

2. Descriptions of the characteristics of the guardrail

The guardrail subject of this work belongs to those designed with the criterion of strength and in Fig. 2 its geometry is reported. The guardrail is formed by a W-beam about 20 cm high and by a secondary beam, 6 cm high, having the function of handrail. The two beams are supported by a series of support posts having a C-section and positioned every 2.4 m. The

Fig. 1. Photos of the accident site (above), of the support guardrail posts (bottom left) and image in detail of a severe deterioration at the base of a post (right).

longitudinal continuity of beams is guaranteed by a bolted joint, while a second bolted joint between the beams and the support posts guarantees the maintenance of the vertical position of the W-beams.

With regard to the steel material, in the absence of reliable data, it has been assumed as a Fe360, (today called S235, $f_{yk} = 235\ \mathrm{N/mm^2}$; $f_{uk} = 360\ \mathrm{N/mm^2}$) widely used at the time of the installation of the structure.

At the base of support posts, as highlighted in Fig. 1, there is a state of deterioration by corrosion that reduces the resistant section of the post. From the statistical point of view, out of 50 posts examined 32 posts seemed to be in good conditions, 14 with an evident state of deterioration and 2 posts strongly deteriorated (one of them is shown on the right side of Fig. 1). Unfortunately it is not possible to determine the condition of deterioration of the two posts involved in the accident since the violent impact and the subsequent collapse of the posts made it difficult to interpret the actual state of the posts involved. For this reason, in order to examine the influence of the state of deterioration at the base of the post on the dynamics of the accident, a state of conventional deterioration was assumed reducing the thickness in a uniform manner, from the design value of 3.5 mm to a value of 1 mm.

3. Qualitative reconstruction of the dynamics of the impact

Since the ultimate strength of guardrail depends on the mechanism of collapse that occurred, first of all we examined the dynamics of the collapse with the aim of understanding the structural behaviour of the guardrail during the impact. Afterwards, on the basis on the evidence presented in this section, we will assess the strength of the guardrail.

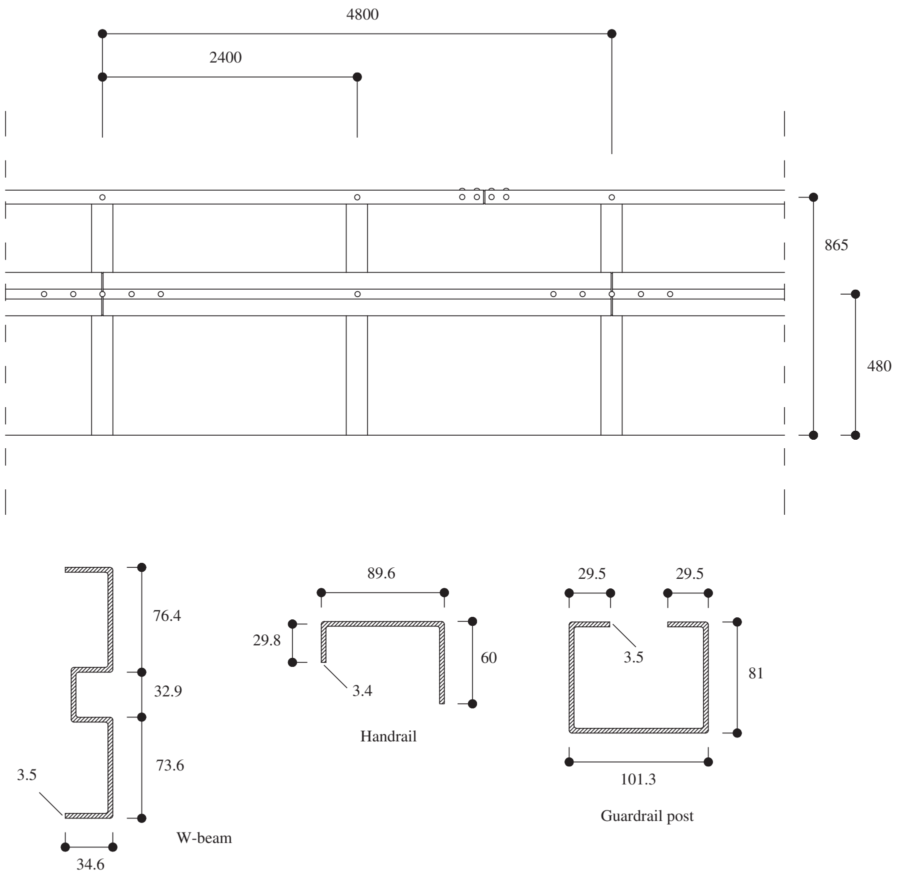

Fig. 2. Geometric dimensions of the elements of the guardrail (mm).

Fig. 3 shows the side of the accident photographed during the recovery operations of the vehicle. Using a drawing software, part of the guardrail that had collapsed was virtually reconstructed in its original location. With the letters B, C, D the three support posts involved in the impact are indicated. The braking points show how the vehicle impacted on the guardrail with the right front side almost at the support post indicated by the letter C.

The dynamics of the impact are reconstructed in a qualitative manner in Figs. 4 and 5. Fig. 4a shows the approach of the vehicle to the guardrail when the driver realises that he is no longer able to control the vehicle at the bend and starts to brake abruptly.

The two thick lines in the figure represent the traces of braking in the same position that can be deduced from Fig. 3. The violent braking causes the loss of grip between the wheels and the asphalt with the subsequent loss of manoeuvrability of

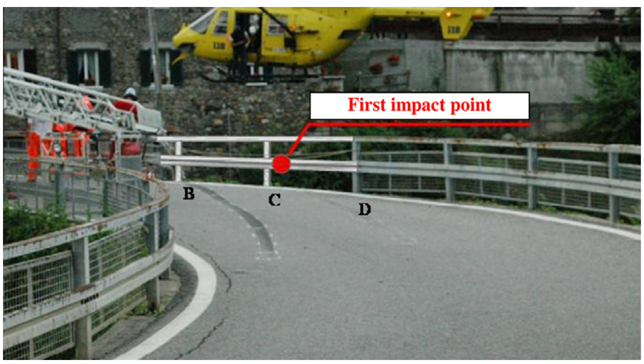

Fig. 3. Virtual reconstruction of the guardrail and assessment of the point of first impact.

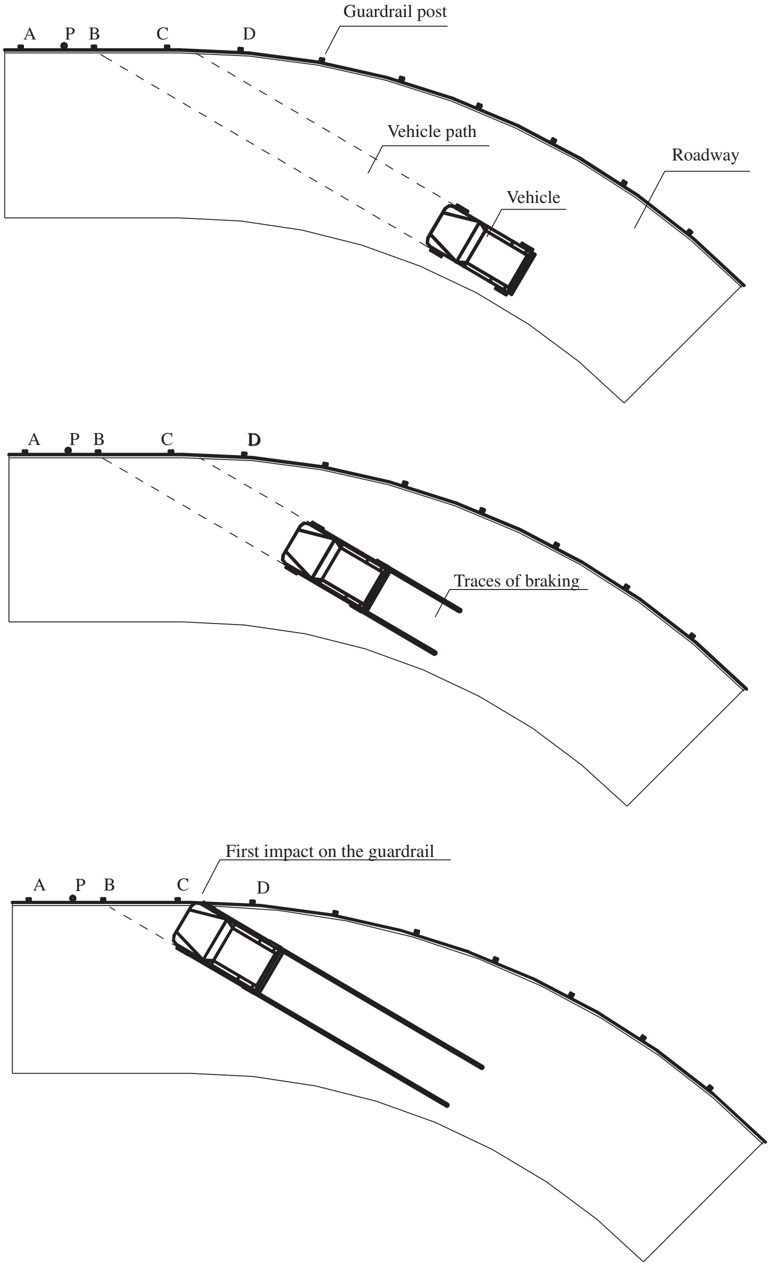

Fig. 4. Virtual reconstruction of the phases of the accident and collapse of the guardrail.

the vehicle that is launched against the guardrail (Fig. 4b). The impact between the vehicle and the guardrail occurred close to the support post C, a few centimetres to the right of the same (Fig. 4c).

The sudden impact probably caused an immediate local deformation of the guardrail. Given the close position of the impact to post C, the guardrail initially offered a resistance according to the strength of the post, dissipating only a small quantity of kinetic energy of the vehicle. Fig. 5a shows the probable configuration of the guardrail system – vehicle at this moment. As the resistance offered by the post it is only a small part of the global resistance of the guardrail, the base of the post C soon reached the condition of collapse, probably when the other structural parts had still not undergone deformation in order to be able to intervene with a "rope" mechanism.

Having still almost entirely its kinetic energy, the vehicle continues on its way veering off the roadway and deforming the W-beam of the guardrail about 1 m in transversal direction. The main belt of the guardrail undergoes a large deformation, resisting in deformed position through an action of axial compression provided from the BC, and a tensile force, provided from the side CD (Fig. 5b). Such resistant mechanism is the main resistant mechanism of the guardrail that can only occur

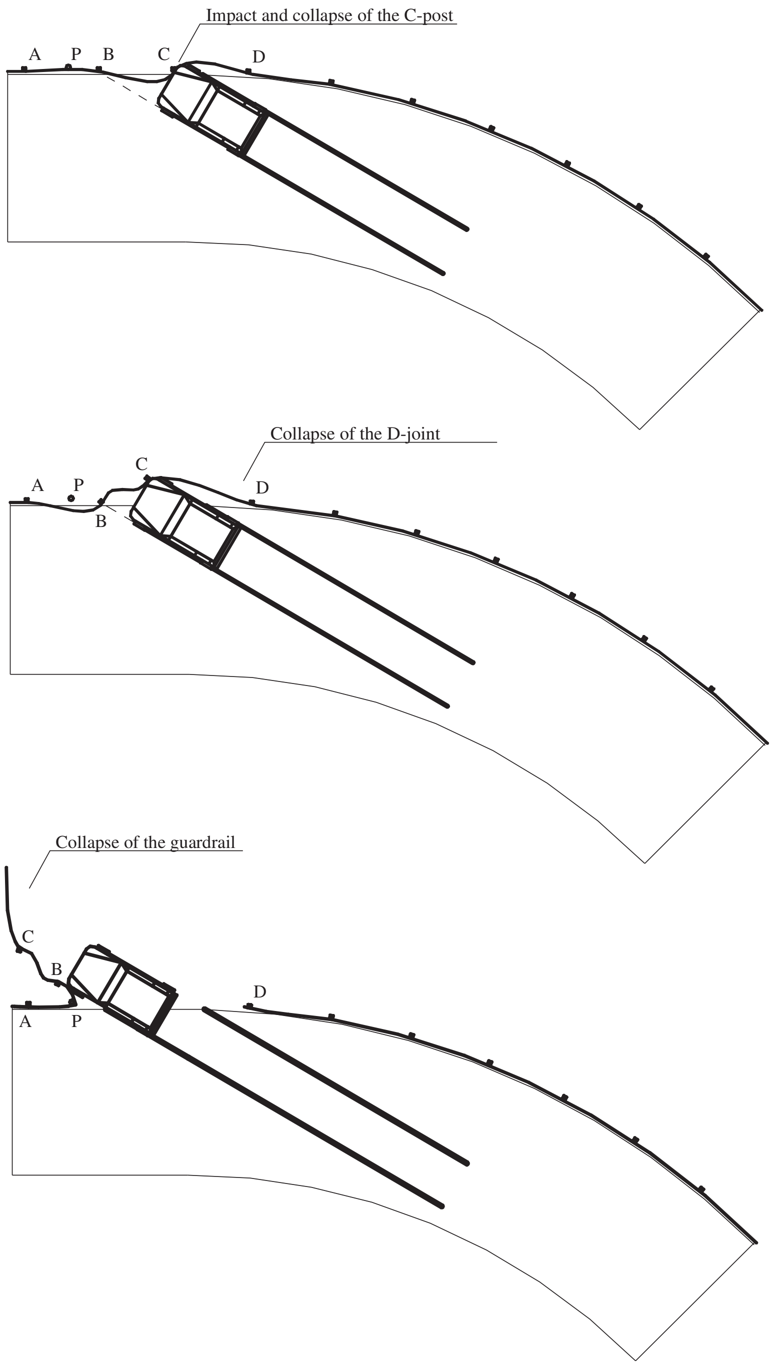

Fig. 5. Virtual reconstruction of the phases of the accident and the collapse of the guardrail.

under great deformations and it is evidenced by the plastic deformation found on the W-beam of the guardrail after the accident.

Fig. 6 shows plastic deformations present on the main W-beam of the guardrail after the collision. The figure on the left shows the segment BC, that is the segment on the left hand side of the point of impact. Such part shows a clear sinusoidal deformation that suggests the absence, at the time of collapse, of an axial tensile force. The segment on the right hand side instead appears in different conditions (the CD segment can be seen in Fig. 6 on the right) that seems to be rectilinear, as if during the collapse it had been only subject to strong traction force.

Fig. 6. Plastic deformations or deteriorations present on the main bend. On the left part BC, on the right part CD.

The strong traction present in the CD segment of the W-beam of the guardrail caused the collapse of the bolted joint in D due to plate bearing failure. Fig. 7 on the left shows traces of bearing action on the W-beam of the CD part. It should be noted how the fixing holes of bolts, initially of 2 cm in diameter measured up to 5 or 6 cm. Fig. 7 on the right shows the joint of the W-beam on the right of the CD segment and not directly involved in the collision. It should be noted that two years after the accident a bolt, that had wedged into the plate during the collapse of the joint, is still visible.

Moving the plasticized steel at the side of the bolt, the bearing action caused strong axial traction in the bolts of the joint that has caused the failure of the bolts due to the loss of the lock nut. The guardrail, devoid of the resistant action of the D joint, opened up as shown in Fig. 5c causing the vehicle to jump off the road and the subsequent impact against the slope of a mountain.

Afterwards the guardrail revolves around a power pole located near the B point and remains suspended from the joint in B. Since there is no evidence of other plastic deformations, it is excluded that the vehicle, in its fall trajectory, had struck the power pole.

Virtually elaborating some images, we are able to reconstruct in Fig. 8 the deformation of the guardrail and the qualitative position of the vehicle at the time of the collapse of joint D.

From the reconstruction of Fig. 8 two important information can be inferred. Even by offering a little strength, the guardrail post positioned in C contributed to the vehicle braking. In fact, if the pole in C had had a zero resistance, the local deformation of the guardrail in C would have been different and it would not have shown the change of curvature that is evident in Fig. 8. Moreover, considering unimportant the axial plastic deformation present in the guardrail and knowing the distance between the two support poles, from Fig. 8 it is possible to deduce that at the moment of the collapse of the joint in D the guardrail showed a central shift of about 1 m.

4. Quantitative assessment of the dynamics of the impact

Based on the evidence presented in the previous section, we are now addressing the quantitative reconstruction of the dynamics of the impact. Through this evaluation we aim to estimate the speed of the vehicle at the entrance to the bend as well as the ultimate strength of the guardrail. In order to obtain this evaluation we can use different methods. For instance it is possible to model the impact through a finite element software in non-linear dynamics and to proceed to identify, solving an inverse problem, the resistances, the damage, and the other variables of interest on the basis of known data [2,10]. However, analysis of this kind introduces much uncertainty in modelling [31] that cannot be easily managed, especially if

Fig. 7. Detail of the collapse due to plate bearing stress in the D joint. On the left the part of joint belonging to the CD segment, on the right the part of joint that remained in situ.

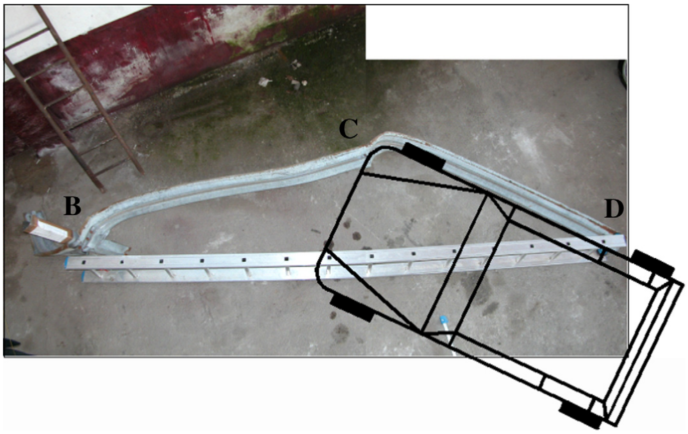

Fig. 8. Qualitative reconstruction of the position of the vehicle and of the plastic deformation of the guardrail at the time of collapse of joint D.

the analysis is performed years after the accident and many information have been lost. In forensic environment, we are preferred not to introduce complex numerical modelling but to reconstruct the dynamics of the accident through a backwards step-by-step process, using simple and well-established physical laws and reducing the use of numerical modelling. As such, the dynamic of the accident is reconstructed through the following guidelines.

We indicate with V_6 the moving speed of the vehicle at the entrance to the bend when the driver notices the danger and stops accelerating to start to brake. The action is not instantaneous but requires a certain time interval that depends mainly on the conditions of physical and mental alertness of the driver. In this period of time (generally between 0.5 and 2 s) the vehicle undergoes a decrease in speed due to the braking action of the engine. Then the speed passes from value V_6 to V_5. Subsequently the energy action of braking changes the speed from value V_5 to value V_3 in a time interval in which the wheels leave signs of braking on the asphalt. The value V_3 is therefore the speed of first impact on the guardrail. The vehicle impacts with the front side close to the support post C causing its collapse. The energy required to break the post leads in a further decrease of speed from V_3 to V_2. At this point the guardrail becomes considerably deformed (about 1 m of transversal displacement) and the vehicle brakes until collapse of the D node due to the bearing failure of the bolted joint. At this point the vehicle still has a non-zero speed, that we indicate with V_1, and this is the cause of the jumping of the vehicle off of the road. Finally, the vehicle impacts on the ground and annuls its own speed. Through a backward reconstruction, all speeds indicated will be assessed.

4.1. Speed assessment V_1

The vehicle was found in the bed of the river below the bridge at about 30 m far from the point of impact on the guardrail. This distance was covered by the vehicle in part by an air trajectory and in part by slipping down the slope of the mountain. On the basis of testimonies and surveys, carried out immediately after finding the vehicle, the point of impact of the vehicle was estimated with the side of the mountain at a horizontal distance of approximately 10 m from the point of impact on the barrier. The topographic surveys point to a difference in altitude between these two points of about 9.8 m. Assuming that the vehicle jumped off from the road with a zero vertical speed and assuming that there had not been any loss of energy during the fall trajectory, the time required for the vehicle to impact on the ground can be estimated as:

$$t = \sqrt{\frac{2 \cdot \Delta Y}{g}} = \sqrt{\frac{2 \cdot 9.8}{9.806}} = 1.41 \text{ s} \tag{1}$$

in which with ΔY is indicated the vertical distance covered and with g the acceleration of gravity. Since the vehicle has covered in this fall a horizontal distance of approximately 10 m, the jump speed from the road can be estimated as:

$$V_1 = \frac{\Delta X}{t} = \frac{10}{1.41} = 7.1 \text{ m/s} = 25.6 \text{ km/h} \tag{2}$$

where ΔX indicates the horizontal distance covered during the fall trajectory. The speed V_1 represents the residual speed of the vehicle after the collapse of the guardrail.

4.2. Speed assessment V_2

To assess speed V_2 it is necessary to consider the braking action exerted by the guardrail during the impact with the vehicle. During this phase the support pole C broke at its basis and the braking action was only given by the deformation in large movements of the W-beam. The decrease of speed of the vehicle resulting from this braking action can be estimated according to the well knew Impulse-Momentum Theorem synthetised by Eq. (3):

$$F \cdot \Delta T = M \cdot \Delta V \tag{3}$$

in which F is a force applied to a mass body M for a time ΔT and ΔV which represents the variation of speed over time. In the case analysed, force F is represented by the force of the impact, that is the force that the barrier transmits to the impacting vehicle. Such force cannot be greater than the value that causes the guardrail collapse. Based on the geometric configuration of collapse that can be inferred in Fig. 7 it is possible to determine, through a simple numerical static field, the relationship existing between the force of impact F and the axial action of joint D that causes breakage of the joint (Fig. 9).

Fig. 9 shows the numerical model used in which the W-beam is modelled with beam finite elements and the stiffness of the guardrail posts are modelled with equivalent elastic springs. At the point of application of the force, springs have not been inserted because the guardrail post C is considered broken. The numerical model indicates that if the impacting force has a value equal to 1, the axial action in the joint D is 0.79.

Using the geometries shown in Fig. 1 the axial action in the CD segment that causes the collapse of the guardrail is estimated to be 115,540 N (assessed by adding the bearing strength of bolts in the W-beam, the shear strength of the bolts in the handrail and tensile strength of a secondary element present in the joint), thus an estimation of the impacting force F is obtained equal to 146,000 N. The Impulse-Momentum Theorem now allows evaluation of the variation of speed experienced by the vehicle. Introducing an appropriate correction factor K, Eq. (3) provides:

$$\Delta V = K \cdot \frac{F \cdot \Delta T}{M} \tag{4}$$

The Impulse-Momentum Theorem provides the variation in speed of a body with mass M subject to a force F, constant for a period interval of ΔT. In the case analysed the force F is not constant, but changes from an initial minimum value to a final maximum value. The minimum initial value is the value of the force that causes the break of the guardrail post C while the maximum final value corresponds to the value that leads to the collapse the structural system. Since in the moments prior to collapse the steel is plasticised, the maximum force applied will be, even if for a short period, constant over time. It is reasonable, therefore, to assume that the correction coefficient K has a value of between 0.5 and 1 and as such a value equal to 2/3 was used.

With regard to the time interval ΔT to be used in Eq. (4), a value equal to 0.15 s was estimated which is reasonably the time required by the vehicle to move transversely of about 1 m at the speed considered. Taking into account that the impacting vehicle has a mass M equal to 1350 kg, the following is obtained:

$$\Delta V = \frac{2}{3} \cdot \frac{146,000 \cdot 0.15}{1350} = 10.8 \text{ m/s} = 38.9 \text{ km/h} \tag{5}$$

Since the vehicle has a residual speed (after collapse of the barrier) equal to 7.1 m/s, the speed of impact V_2 is:

$$V_2 = 7.1 + 10.8 = 17.9 \text{ m/s} = 64.4 \text{ km/h} \tag{6}$$

This value represents the speed that the vehicle has during the impact, before significant deformation of the guardrail takes place and after the collapse of the guardrail post C.

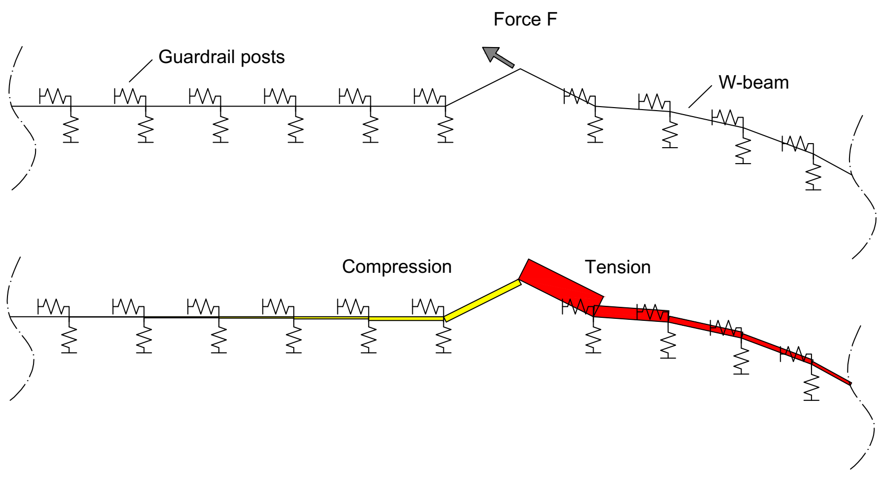

Fig. 9. Numerical model and axial stresses in the guardrail.

4.3. Speed assessment V_3

To evaluate the speed of the vehicle before the collapse of the guardrail post C, it is necessary to use a second numerical model. In this case the guardrail is assumed to be not deformed (Fig. 10) and the guardrail post C is modelled using elastic springs similar to the other support posts. In order to model a serious state of corrosion at the base of the guardrail post, the design thickness (3.5 mm) is evenly reduced to 1 mm. If the impacting force has a value of 1, the numerical model provides, on the guardrail post C, a force equal to 0.1 in a longitudinal direction and 0.5 in a transversal direction.

By performing an assessment through biaxial bending formulas, it is estimated that for an impacting force of 753 N the collapse of the guardrail post is obtained. At this point, using again the Impulse-Momentum Theorem, the decrement of speed during the collapse of the guardrail post C is assessed as:

$$DV = K \times \frac{F \times DT}{M} = \frac{2}{3}\frac{753 \times 0.015}{1350} = 0.056 \text{ m/s} \tag{7}$$

Therefore, the speed of impact on the guardrail V_3 is:

$$V_3 = 17.9 + 0.056 = 18.0 \text{ m/s} = 64.8 \text{ km/h}. \tag{8}$$

4.4. Speed assessment V_6

The speed with which the driver entered the bend will undoubtedly be greater than the speed of impact on the barrier estimated in the previous section, due to the loss of speed due to braking. The action of braking can be divided into two parts: the braking action due to sliding friction that occurs when the wheels of the vehicle are locked and that due to rolling friction (that occurs before the wheels lock). Assuming a friction coefficient of $f = 0.50$ (rubber – asphalt in humid conditions) through an energy balance it is possible to estimate the speed of the vehicle at the time of starting of sliding friction:

$$\frac{1}{2} \cdot M \cdot V_3^2 + M \cdot g \cdot f \cdot s = \frac{1}{2} \cdot M \cdot V_4^2 \tag{9}$$

$$V_4 = \sqrt{V_3^2 + 2 \cdot g \cdot f \cdot s} = \sqrt{18.0^2 + 2 \cdot 9.806 \cdot 0.85 \cdot 12.30} = 21.1 \text{ m/s} = 76.0 \text{ km/h} \tag{10}$$

in which g is the gravitational acceleration (9.806 m/s^2) and s is the length of braking that can be deduced from the marks on the asphalt (12.30 m).

Assuming that the rolling friction took place for a short fraction of time (0.2 s) the speed of the vehicle at the start of braking can be estimated as:

$$V_5 = V_4 + t_v \cdot (g \cdot f_v + d_m) = 21.1 + 0.2 \cdot (9.806 \cdot 0.55 + 1) = 22.4 \text{ m/s} = 80.6 \text{ km/h} \tag{11}$$

where a coefficient of rolling friction (f_v) equal to a 0.55 has been assumed while braking action of the engine (d_m) was assumed to be 1 m/s^2.

To this speed, a further increase must be added, due to the braking action of the engine that occurred between the time in which the driver removed his feet from the accelerator and the time when he started to brake. Such time interval (t_p), depends on the reactive capabilities of the driver. Depending on the data available from the forensic survey, a reaction time of 2 s is estimated. The initial speed of the vehicle, entering the bend, and before braking is thus evaluated as:

$$V_6 = V_5 + t_p \cdot d_m = 22.4 + 2 \cdot 1 = 24.4 \text{ m/s} = 87.8 \text{ km/h} \tag{12}$$

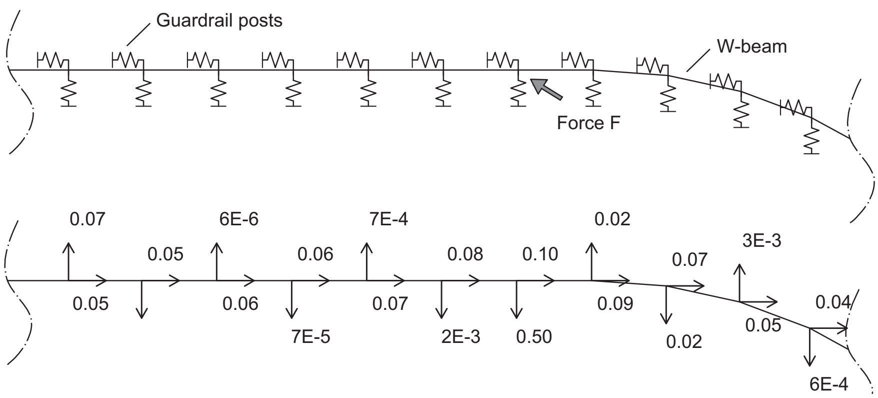

Fig. 10. Numerical model of the guardrail before the impact and assessment of the forces on the guardrail post C.

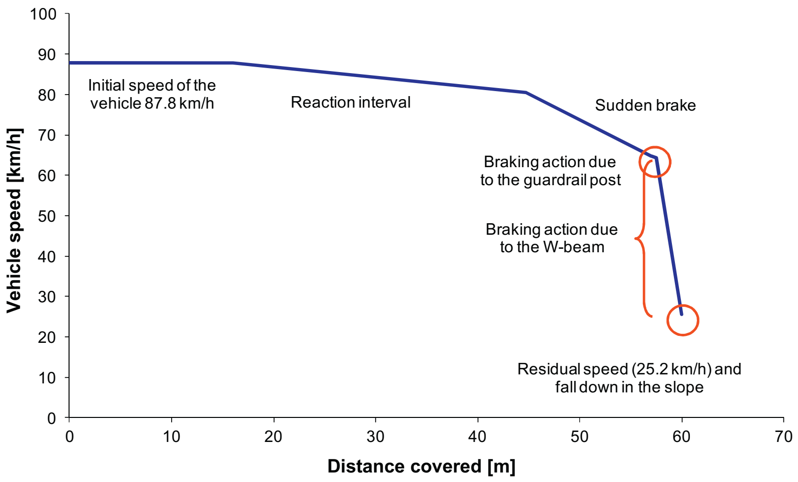

Fig. 11. Diagram of the speed variation of the vehicle from the moment of entering into the bend until collapse of the guardrail (thickness of the deteriorated support pole C).

Fig. 11 shows the values of speed evaluated in these sections. As can be seen from the diagram, the vehicle is subject to two significant decreases of speed: the first one during the abrupt braking and the second due to the resistant mechanism of the W-beam. In terms of reduction of speed the contribution guardrail post C is negligible.

5. Quantitative estimation of the dynamics of the impact in conditions of absence of deterioration

In the previous section the variation of speed of the vehicle during collision with the guardrail was evaluated, assuming that the guardrail post was affected by a conventional deterioration (reduction of thickness from 3.5 mm to 1.0 mm evenly on the section). The same evaluations can be referred to a guardrail in perfect conditions of service (thickness of the guardrail post C equal to the design thickness of 3.5 mm). Considering the same hypotheses assumed in the previous section and starting from a speed of 87.8 km/h a speed of exit from the road of 25.2 km/h can be obtained against the 25.6 km/h estimated with the guardrail post in deteriorated conditions. The influence of the state of deterioration at the base of the guardrail post C is thus minimal, not influencing the dynamics of the accident or the mode of collapse of the guardrail.

6. Evaluation of resistance that the guardrail should have had to stop the vehicle

Based on the previous evaluations, it is finally possible to estimate the resistance that the bolted joint should have had to stop the vehicle on the road. Considering the speed of impact V_3 of 17.9 m/s and assuming a zero speed of the vehicle at the time of collapse of the joint due to bearing action, the Impulse-Momentum Theorem provides a force of impact of:

$$F = K \cdot \frac{\Delta V \cdot M}{\Delta T} = \frac{3}{2} \cdot \frac{17.9 \cdot 1350}{0.15} = 241,650 \text{ N} \quad (13)$$

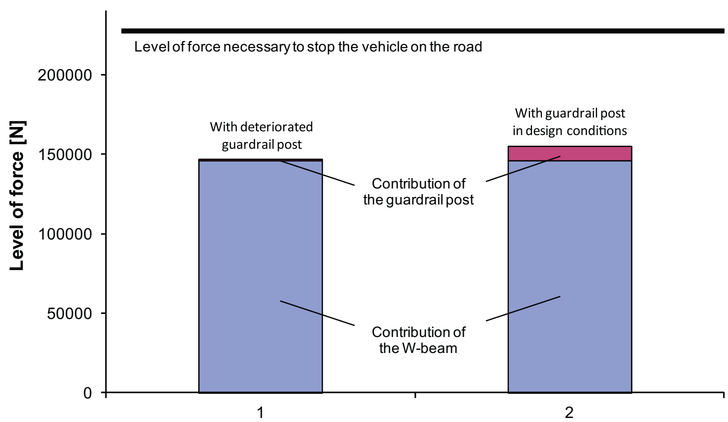

Fig. 12. Resistance offered by the guardrail. The histogram 1 is refers to the barrier with the guardrail post conventionally deteriorated (thickness of 1 mm) while the histogram 2 refers to the design situation (thickness of 3.5 mm). The black line represents the threshold of resistance necessary to stop the vehicle on the road.

greater than the estimation of the force that caused the collapse of the barrier (approximately 150,000 N). The histogram of Fig. 12 compares the contributions to the resistance offered by various resistant mechanisms during the impact. The histogram on the left refers to the barrier with the guardrail post conventionally deteriorated (thickness of 1 mm) while the histogram on the right refers to the design situation (thickness of 3.5 mm).

From the comparison of Fig. 12, the resistance offered by the support post C in design conditions (absence of deterioration) can be quantified as 6% of the total resistance of the guardrail. In conditions of conventional assumed deterioration, the resistance of the support post C contributes 1%. Therefore, the conventional deterioration assumed caused a loss of only 5% on the total resistance of the guardrail.

7. Conclusions

In this work we have analysed the collapse behaviour of a guardrail with signs of corrosion at the base of a support post. It was necessary to study this subject, after a vehicle veered off a road leading to the collapse of the guardrail. Through reconstruction of the dynamics of the impact, the speed of the vehicle was estimated of approximately 87.8 km/h over a stretch of road where the mandatory speed limit is 30 km/h. The driver therefore lost control at a very narrow bend just before a bridge, impacting violently against the guardrail. The barrier reacted to the force of the veering vehicle with a remarkable transversal action but collapsed due to the violence of the collision thus showing a failure due to the bearing action in the joint. The collapse of the guardrail post, swept away from the vehicle, took place almost immediately. Based on the estimations presented, the resistance of the support post played an absolutely marginal role to the global resistance of the guardrail (approximately 6%). The conventional corrosion assumed at the base of the post led to a reduction of 5% of global resistance of the guardrail. In absence of corrosion at the base of the post, the same would in any case have collapsed and the dynamics of the accident would not have changed (the car would have jumped off the road at 25.2 km/h instead of 25.6 km/h). The level of corrosion noted on site was thus insufficient to cause a loss of functionality of the guardrail, and this was because the guardrail was still able to perform its function of restraint, deforming in significant displacements until collapse due to bearing stress.

Acknowledgements

The author wishes to thank the Province of Verbano-Cusio-Ossola, the Eng. Giandomenico Vallesi and the Prof. Pier Giorgio Malerba for their useful suggestions provided. A special thanks to Dr. Naomi Basso.

References

[1] American Association of State Highway and Transportation Officials. Roadside design guide. Roadside barrier. Washington, DC: AASHTO; 2002 [chapter 5].
[2] Arangio S. Back analysis of structural model parameters: the application of neural networks. In: Proceedings of the 5th international conference on engineering computational technology, ECT 2006, Las Palmas de Gran Canaria, Spain; 12 September 2006–15 September 2006. 13p.
[3] Atahan AO. Finite element simulation of a strong-post W-beam guardrail system. Simulation 2002;78(10):587–99.
[4] Atahan AO, Cansiz OF. Impact analysis of a vertical flared back bridge rail-to-guardrail transition structure using simulation. Finite Elem Anal Des 2005;41:371–96.
[5] Atahan AO, Yücel AÖ, Erdem MM. Crash testing and evaluation of a new generation L1 containment level guardrail. Eng Fail Anal 2014;38:25–37.
[6] Barbato M, Petrini F, Unnikrishnan VU, Ciampoli M. Performance-based hurricane engineering (PBHE) framework. Struct Saf 2013;45:24–35.
[7] Binda L, Lualdi M, Saisi A, Zanzi L. Radar investigation as a complementary tool for the diagnosis of historic masonry buildings. Int J Mater Struct Integrity 2011;5(1):1–25.
[8] Bontempi F, Giuliani L, Gkoumas K. Handling the exceptions: robustness assessment of a complex structural system. Struct Eng Mech Comput (SEMC), Cape Town, South Africa 2007;3:1747–52.
[9] Ciampoli M, Petrini F, Augusti G. Performance-based wind engineering: towards a general procedure. Struct Saf 2011;33(6):367–78.
[10] Crosti C, Bontempi F. Back-analysis of the collapse of a metal truss structure. In: Research and applications in structural engineering, mechanics and computation – proceedings of the 5th international conference on structural engineering, mechanics and computation, SEMC; 2013. p. 2401–6.
[11] Coon BA, Reid JD. Reconstruction techniques for energy-absorbing guardrail end terminals. Accid Anal Prev 2006;38(1):1–13.
[12] Daniello A, Gabler HC. Effect of barrier type on injury severity in motorcycle-to-barrier collisions in North Carolina, Texas, and New Jersey. Transp Res Rec 2011;2262:144–51.
[13] Giuliani L, Prisco V. Nonlinear analysis for progressive collapse investigation on reinforced concrete framed structures. In: Proceedings of the 2008 structures congress – structures congress 2008: crossing the borders; 2008. p. 314.
[14] Elvik R. The safety value of guardrails and crash cushions: a meta-analysis of evidence from evaluation studies. Accid Anal Prev 1995;27(4):523–49.
[15] European Committee for Standardization. EN 1317-4 impact test acceptance criteria and test methods for terminals and transitions of safety barriers. European Committee for Standardization; 2002.
[16] European Committee for Standardization. EN 1317-2 performance classes, impact test acceptance criteria and test methods for safety barriers and vehicle parapets. European Committee for Standardization; 2005.
[17] Ferdous MR, Abu-Odeh A, Bligh RP, Jones HL, Sheikh NM. Performance limit analysis for common roadside and median barriers using LS-DYNA. Int J Crashworthiness 2011;16(6):691–706.
[18] Ibitoye AB, Hamouda AMS, Wong SV, Radin RS. Simulation of motorcyclist's kinematics during impact with W-Beam guardrail. Adv Eng Softw 2006;37:56–61.
[19] Lambert JH, Baker JA, Peterson KD. Decision aid for allocation of transportation funds to guardrails. Accid Anal Prev 2003;35(1):47–57.
[20] Lampo RG, Johnson HE, Olaes C, Palutk K. Investigation of corrosion-resistant materials for security fencing and personnel handrails. In: Corrosion conference, La Quinta, California; 2011.
[21] Leopardi S, Pappalardo G. Analisi critica delle caratteristiche prestazionali delle barriere di sicurezza, Quaderno 110. Istituto di Strade Ferrovie Aeroporti, Università degli Studi di Catania; 2000 [in Italian].
[22] Long K-J, Li Y, Lei Z-B, Zheng J-L. Evaluating roadside hazard rating based on acceleration severity index. Zhongguo Gonglu Xuebao/China J Highway Transp 2013;26(3):143–59.

[23] Lualdi M, Lombardi F. Effects of antenna orientation on 3-D ground penetrating radar surveys: an archaeological perspective. Geophys J Int 2013;196(2):818–27.
[24] Olmati P, Gkoumas K, Brando F, Cao L. Consequence-based robustness assessment of a steel truss bridge. Steel Compos Struct 2013;14(4):379–95.
[25] Petrini F, Ciampoli M. Performance-based wind design of tall buildings. Struct Infrastruct Eng 2012;8(10):954–66.
[26] Polivka KA, Sicking DL, Rohde JR, Faller RK, Holloway JC. Crash testing of Michigan's type B (W-Beam) guardrail system. MwRSF research report TRP-03-90-99. Lincoln, NE: University of Nebraska; 1999.
[27] Polivka KA, Sicking DL, Rohde JR, Faller RK, Holloway JC. Crash testing of Michigan's type B (W-beam) guardrail system – phase II. MwRSF research report TRP-03-104-00. Lincoln, NE: University of Nebraska; 2000.
[28] Reid JD, Kuipers BD, Sicking DL, Faller RK. Impact performance of W-beam guardrail installed at various flare rates. Int J Impact Eng 2009;36:476–85.
[29] Ross Jr HE, Krammes RA, Sicking DL, Tyer KD, Perera HS. Traffic barriers and control treatments for restricted work zones. National Cooperative Highway Research Program report 358. Washington, DC: Transportation Research Board; 1994.
[30] Soltani M, Moghaddam TB, Karim MR, Sulong NHR. The safety performance of guardrail systems: review and analysis of crash tests data. Int J Crashworthiness 2013;18(5):530–43.
[31] Sgambi L. Handling model approximations and human factors in complex structure analyses. In: Proceedings of the 10th international conference on civil, structural and environmental engineering computing, civil-comp; 2005. p. 20.
[32] Sgambi L, Bontempi F, Garavaglia E. Structural response evaluation of two-blade bridge piers subjected to a localized deterioration. In: Proceedings of the 3rd international conference on bridge maintenance, safety and management – bridge maintenance, safety, management, life-cycle performance and cost; 2006. p. 153–4.
[33] Sgambi L, Bontempi F, Garavaglia E. Structural response evaluation of two-blade bridge piers subjected to a localized deterioration. In: Proceedings of the third international conference on bridge maintenance, safety and management (IABMAS06), Porto (Portugal); 2006.
[34] Sgambi L, Malerba PG, Gotti G, Ielmini D. The influence of degradation phenomena on collapse modes in prestressed concrete beams. Int J Lifecycle Perform Eng 2012;1(1):41–63.
[35] Tomasch E, Sinz W, Hoschopf H, Gobald M, Steffan H, Nadler B, et al. Required length of guardrails before hazards. Accid Anal Prev 2011;43:2112–20.
[36] Valente M. Seismic protection of R/C structures by a new dissipative bracing system. Proc Eng 2013;54:785–94.
[37] Wu W, Thomson R. A study of the interaction between a guardrail post and soil during quasi-static and dynamic loading. Int J Impact Eng 2007;34:883–98.
[38] Ren Z, Vesenjak M. Computational and experimental crash analysis of the road safety barrier. Eng Fail Anal 2005;12(6):963–73.